



Role of background observed in aptasensor with chemiluminescence detection

Lucienne Park^{a,b,1}, Julie Kim^{a,c,1}, Ji Hoon Lee^{a,*}

^a Luminescent MD, LLC, Hagerstown, MD 21742, United States.

^b Department of Biology, University of Maryland, College Park, MD 20742, United States

^c Thomas Jefferson High School for Science and Technology, Alexandria, VA 22312, United states

ARTICLE INFO

Article history:

Received 1 July 2013

Received in revised form

29 July 2013

Accepted 29 July 2013

Available online 2 August 2013

Keywords:

Aptamer

Aptasensor

Chemiluminescence

Background

Microfibers

Nanoparticles

ABSTRACT

One-step chemiluminescent aptasensor was developed using chemically initiated electron exchange luminescence (CIEEL) between high-energy intermediate formed from 1,1'-oxalyldiimidazole chemiluminescence (ODI-CL) reaction and G-quadruplex (ochratoxin A (OTA)-bound aptamer conjugated with TEX615) generated. The sensitivity of chemiluminescent aptasensor, optimized with various variables (e.g., property of microfibers fabricated with 3,4,9,10-perylene-tetracarboxylic dimide, determination of fluorescent dye labeled with aptamer, physical properties of buffer solution), was dependent on the background (concentration of high-energy intermediate) generated in ODI-CL reaction. The limit of detection (LOD = background + 3 × standard deviation, 0.5 nM) of ODI-CL aptasensor with lower background was lower than that (3.7 nM) with 20 times higher background. Also, the ratio of signal to background (S/B) of ODI-CL aptasensor with low background was about 5-fold higher than that with high background. The sensitivities of ODI-CL aptasensors, with low as well as high background, capable of accurately and precisely quantifying OTA within 10 min, were better than those of fluorescent aptasensors and as good as those of highly sensitive but time-consuming competitive enzyme-linked immune-sorbent assays (ELISAs) using expensive antibody produced with the sacrifice of small animals.

© 2013 Elsevier B.V. All rights reserved.

1. Introduction

The development of various DNA- and RNA-aptamers to bind specific target molecules has led to the design of a variety of aptasensors using optical detection (e.g., absorbance, chemiluminescence, fluorescence) to rapidly monitor environmental toxicants [1] and to early diagnose/prognose various diseases [2]. Aptasensor development is promising because they are expected to be more rapid and cost-effective than immunoassays, which are complicated, time-consuming and use expensive antibodies and enzymes. However, the accuracy, precision and sensitivity of aptasensors still need to be improved so that they are as good as, or better than, immunoassays.

Recently, it was reported that aptamer-conjugated fluorescent dye (ACFD) can be immobilized on the surface of carbon-based nanoparticles (e.g., carbon nanotubes, graphene oxides) [1–3] and microfibers (e.g., 3,4,9,10-perylene-tetracarboxylic dimide microfibers, PDIMFs) [4] due to the π - π stacking interaction between aptamer and nanoparticles as shown in Fig. 1. When the

immobilized ACFDs are added to samples containing the target analytes, the ACFDs rapidly detach from the nanoparticles or microfibers to bind the analytes [1–4]. ACFDs bound with analytes emit fluorescence, whereas ACFDs immobilized on the surface of the nanoparticles emit no fluorescence due to the fast fluorescent resonance energy transfer (FRET) from ACFDs to nanoparticles or microfibers [1–4]. Based on this principle, fluorescence aptasensors were developed to rapidly quantify analytes without the time-consuming procedures (e.g., multiple-time washings and incubations) necessary for immunoassays [5–7]. Unfortunately, the accuracy, precision and sensitivity of fluorescence-based aptasensors [1,2] generally are not as good as those of immunoassays [5–7], primarily because of the high background signal [1,2] that results from light scattering and/or the high voltage power supply needed to generate an intense light source (e.g., laser, Xenon) [8]. Thus, the fluorescence of ACFD bound with trace levels of analyte is often too low to detect using fluorescence. Another critical problem of fluorescent aptasensors is that they need to be used with a low concentration of ACFD and nanoparticles because nanoparticles such as carbon nanotubes are strong quenchers in fluorescence detection systems [2]. Thus, high backgrounds and low signal to background (S/B) ratios often result in calibration curves that are too narrow and inaccurate using fluorescent aptasensors [1–3].

* Corresponding author. Fax: +1 301 393 9092.

E-mail address: jhlee@luminescentmd.com (J.H. Lee).

¹ Lucienne Park and Julie Kim contributed equally in this research.

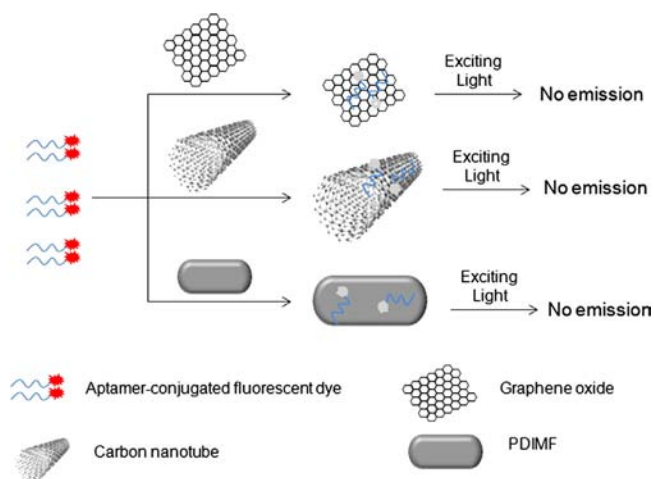
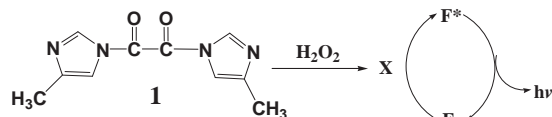


Fig. 1. π - π stacking interaction between aptamer-conjugated fluorescent dye and carbon nano- and micro-particles such as graphene oxide [1], carbon nanotube [2], PDIMF [4].



Scheme 1. ODI-CL reaction. 1: ODI, X: high-energy intermediate formed from ODI-CL reaction, F: fluorescent dye under the ground state, F*: fluorescent dye under the excited state.

N-[(3*R*)-(5-chloro-8-hydroxy-3-methyl-1-oxo-7-isochromanyl) carbonyl]-*L*-phenylalanine (Ochratoxin A or OTA), one of mycotoxins, is known as a toxic contaminant in foods and beverages (e.g., grains, coffee, cocoa, grape juice, wine). Recently, single strand DNA (ssDNA) aptamer capable of specifically binding OTA in a sample was reported [9]. After that, analytical methods for the quantification of OTA [1,2,4,10,11] were developed using OTA aptamer, nanoparticles (e.g., carbon nanotubes, graphene oxide, gold nanoparticles) and various detections such as colorimeter, electrochemical, and fluorescence.

It is well-known that peroxyoxalate chemiluminescence (PO-CL), with low background generated from chemical reactions, can quantify trace levels of fluorescent dyes based on the chemically initiated electron exchange luminescence (CIEEL) mechanism between high-energy intermediate (X) formed in PO-CL reaction and fluorescent dye [12–16]. In particular, one PO-CL reaction, 1,1'-oxalyldiimidazole chemiluminescence (ODI-CL) (Scheme 1), can be used to quantify fluorescent dyes in aqueous solution because the intense CL generated from the ODI-CL reaction has a short life-time and therefore is emitted before the ODI molecules are decomposed in solution [12]. Using the chemical and physical properties of ODI-CL detection, we recently developed highly sensitive and rapid chemiluminescent enzyme immunoassays with ODI-CL detections with excellent accuracy, precision, and recovery [17–20].

Based on the principles of aptasensors using micro- and nanoparticles [1–3] and the advantages of ODI-CL detection [14,17–20] described above, in this manuscript, we report in detail the role of background to develop aptasensor with chemiluminescent detection capable of quantifying trace levels of OTA in a sample.

2. Experimental

2.1. Chemical and materials

3,4,9,10-perylenetetracarboxylic dimide and ochratoxin A (OTA) and Rhodamine 101 were purchased from Sigma (St. Louis, MO,

USA). An aptamer (5'-GAT CGG GTG TGG GTG GCG TAA AGG GAG CAT CGG ACA-3') selected by Cruz-Aquado and Penner [9] was used in this research (Ref.). Three different aptamers conjugated with 6-FAM (5'-6-FAM-GAT CGG GTG TGG GTG GCG TAA AGG GAG CAT CGG ACA-3', TEX 615 (5'-TEX615-GAT CGG GTG TGG GTG GCG TAA AGG GAG CAT CGG ACA-3'), or Texas Red (5'-TEX Red-GAT CGG GTG TGG GTG GCG TAA AGG GAG CAT CGG ACA-3') purified with HPLC were purchased from Integrated DNA Technologies (IDT, Coralville, IA, USA). COOH functionalized multiwall carbon nanotubes (MWCNT, 20–30 nm) were purchased from Nanomaterial Store (Fremont, CA, USA). Bis(2,4,6-trichlorophenyl) oxalate (TCPO) was purchased from TCI-America (Portland, OR, USA). 4-Methylimidazole (4-MImH, 98%) and dimethyl sulfoxide (DMSO, 99%) were purchased from Alfa Aesar (Ward Hill, MA, USA). Hydrogen peroxide (H₂O₂, 30%) was purchased from Mallinckrodt Chemicals (St. Louis, MO, USA). Water (HPLC grade), PBS buffer solution (pH 7.4, components: 137 mM NaCl, 2.7 mM KCl, and 10 mM phosphate buffer), tetrahydrofuran (THF, HPLC grade), and ethyl acetate (HPLC grade) were purchased from EMD (Billerica, MA, USA). Four different Tris-HCl buffer solutions (pH 7.0, 7.5, 8.0, and 8.5, component: monomethane) were purchased from Teknova (Hollister, CA, USA).

2.2. Preparation of 3,4,9,10-perylenetetracarboxylic dimide fibers (PDIMFs)

PDIMFs were prepared with the modification of method reported by Li and Sun [4]. 3,4,9,10-perylenetetracarboxylic dimide (10 mg) was added in tetrahydrofuran (99.5%, 10 ml). Then, the solution was dispersed with an ultrasonicator (Sonicator Cell Distributor, Heat System-Ultrasonic, Inc.) for 30 min in 1 sec interval. PDIMFs formed in the solution were washed two times with deionized water using a centrifuge (4000 rpm). Finally, the washed PDIMFs were dispersed in PBS buffer (pH 7.4, 5 ml). PDIMFs were stored in a refrigerator (2–8 °C).

2.3. Preparation of aptamer-conjugated TEX 615 immobilized on the surface of PDIMFs

PDIMF stock solution was 5-time diluted in PBS buffer to prepare PDIMF working solution. Working solution (500 μ l) was mixed with 220 nM aptamer-conjugated TEX 615 (500 μ l) in PBS buffer using a 1.5-ml microcentrifuge tube. The mixture was incubated for 30 min at room temperature (21 \pm 2 °C) to immobilize Aptamer-conjugated TEX 615 on the surface of PDIMFs. Then, the stock solution was stored in a refrigerator (2–8 °C) until further use. The stock solution was stable for a month in the refrigerator.

2.4. Measurement of CL emitted from aptasensor

2.4.1. Determination of fluorescent dye labeled with aptamer to develop highly sensitive aptasensor with ODI-CL detection

In order to enhance the sensitivity of aptasensor with ODI-CL detection, we prepared three different aptamers (10 nM) conjugated with 6-FAM, TEX 615, or Texas Red in PBS buffer. Each aptamer (10 μ l) was inserted into a borosilicate test tube (12 \times 75 mm², VWR). The borosilicate test tube was placed in a luminometer (Lumat 9507, Berthold Inc.). H₂O₂ (25 μ l) was injected into the test tube using a syringe pump when the start button of the luminometer was pressed. Then, CL emission was immediately measured for 2 sec with the addition of ODI (25 μ l) in the test tube at room temperature. Each CL spectrum measured for 2 sec with 100 msec interval was compared with other CL spectra to determine appropriate fluorescent dye to develop a highly sensitive aptasensor with ODI CL detection.

2.4.2. Analysis of OTA in 1% red wine diluted in PBS buffer

The stock solution of aptamer conjugated TEX 615 immobilized on the surface of PDIMFs was diluted 80 times in PBS buffer to use as working solution. 100 μ l working solution in a 1.5-ml microcentrifuge tube was mixed with a certain concentration of OTA (100 μ l) in PBS buffer containing 1% red wine. The mixture was incubated for 5 min at room temperature (21 ± 2 °C).

ODI stock solution was prepared from the reaction between 5 μ M TCPO and 20 μ M 4-methylimidazole in ethyl acetate. To quantify OTA under various background conditions, the stock solution was 2-, 20-, and 200-time diluted in ethyl acetate to use as working solution. 0.2 M H_2O_2 working solution was prepared in isopropyl alcohol.

The mixture of standard (or sample) and aptamer conjugated TEX 615 immobilized on the surface of PDIMFs (10 μ l) was inserted into a borosilicate test tube. The borosilicate test tube was placed in the luminometer. H_2O_2 (25 μ l) was injected into the test tube using a syringe pump after the start button of the luminometer was pressed. Then, CL emission was immediately measured for 0.7 sec with the addition of ODI (25 μ l) in the test tube at room temperature.

After measuring CL emitted in mixtures containing different concentrations of OTA using three different ODI working solutions, we studied the sensitivity of the aptasensor. Also, we studied the accuracy, precision, and recovery of the aptasensor with 200-time diluted ODI working solution.

3. Results and discussion

3.1. Determination of fluorescent dye labeled with aptamer to develop highly sensitive aptasensor with ODI-CL detection

6-FAM is widely used as a fluorescent dye conjugated with DNA aptamers to develop fluorescent aptasensors [2]. The quantum efficiencies of Texas Red in conventional PO-CL reaction is much higher than other fluorescent dyes dissolved in aqueous solution [21]. However, Fig. 2 indicates that a more appropriate fluorescent dye labeled with a specific aptamer, capable of capturing ochratoxin (OTA), is TEX 615 synthesized to replace Texas Red by Integrated DNA Technologies (IDT), Inc. Fig. 2 indicates that ODI chemiluminescent aptasensor using OTA aptamer conjugated with TEX 615 can be more sensitive than those using aptamer-conjugated 6-FAM or Texas Red. Fig. 2 shows that quantum efficiency of 6-FAM is slightly better than that of Texas Red in ODI-CL reaction because the property of X formed in ODI CL reaction [13,14] is different from that generated in conventional PO-CL reaction [12]. In addition, Fig. 2(b) shows that the temporal decay in CL resulting from the ODI-CL reaction depends on the the fluorescent dye used. Due to the sensitivity problem of fluorescence, the concentrations of 6-FAM, Texas Red, and TEX 615 used to measure fluorescence were 10 times higher than those to used measure ODI-CL. As shown in Fig. S1 of supporting information, relative fluorescence intensity of 6-FAM was similar to that of TEX 615 whereas that of Texas Red was the lowest.

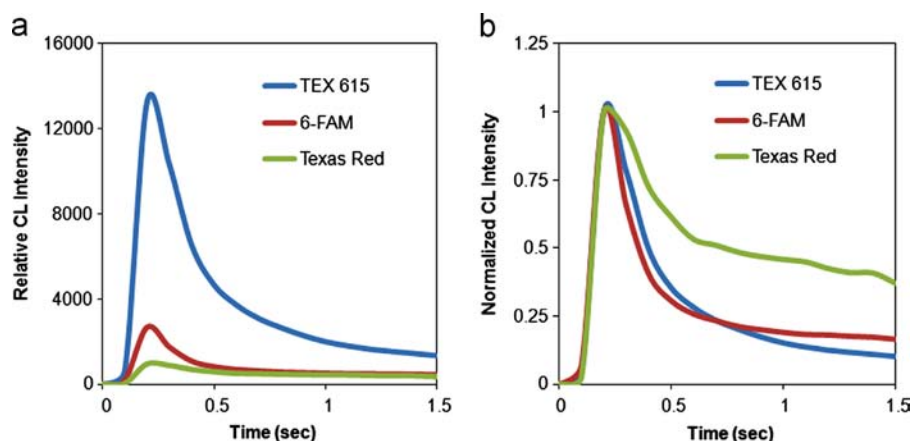


Fig. 2. ODI-CL spectra of three different fluorescent dyes labeled with aptamer capable of capturing OTA. [aptamer-conjugated fluorescent dye]=10 nM in PBS, ODI was formed from the reaction between 5 μ M TCPO and 20 μ M 4-MImH in ethyl acetate, [H_2O_2]=0.2 M in isopropyl alcohol.

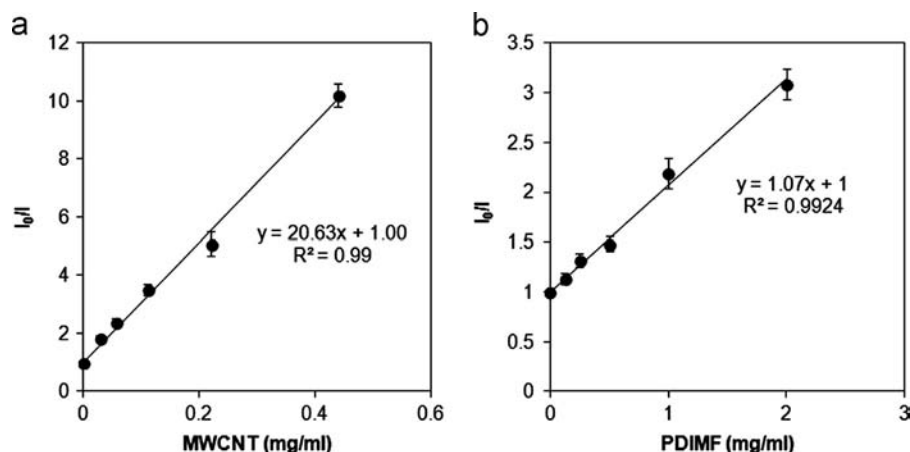


Fig. 3. Quenching effect of MWCNTs (a) and PDIMFs (b) in ODI-CL reaction. [Rhodamine 101]=2.0 nM in PBS, ODI-CL reaction condition was the same as that of Fig. 2.

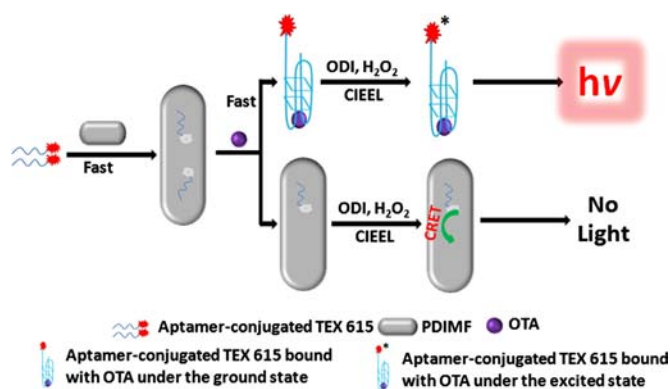


Fig. 4. Basic principle of chemiluminescent aptasensor capable of quantifying OTA.

Table 1

Interaction between aptamer and PDIMF ($n=3$).

	Background ^a	Aptamer ^b only	Incubation of solution containing aptamers ^b and PDIMFs ^c		
			Immediate	2 min	10 min
I_{CL} ^d	1120	271,911	10,693	8915	8329

^a Relative CL intensity (I_{CL}) of PBS buffer containing PDIMF only.

^b [Aptamer-conjugated TEX 615] = 220 nM in PBS.

^c [PDIMF] = 1 mg/ml in PBS.

^d ICL: relative CL intensity integrated for 0.7 sec. The error range of I_{CL} shown in the table was 3–5%.

3.2. Effect of PDIMFs and multi-walled carbon nanotubes (MWCNTs) in ODI-CL reaction

We studied the effect of PDIMFs when fluorescent dyes emit light in ODI CL reaction. We used Rhodamine 101, instead of TEX 615, as a fluorescent dye in this study. This is because the (1) quantum efficiency of Rhodamine 101 in ODI CL reaction is excellent [23] and (2) chemical structure of Rhodamine 101 is similar to that of TEX 615. Unfortunately, we were not able to purchase pure TEX 615 from IDT even though aptamer-conjugated TEX 615 is available.

As shown in Fig. 3(a), multi-walled carbon nanotubes (MWCNTs, 20–30 nm) are a strong quencher in ODI-CL reaction. The result indicates that it is difficult to develop a highly sensitive ODI chemiluminescent aptasensor because S/B ratio is reduced due to the strong quenching of signal by MWCNTs. To solve this problem, we studied the physical property of PDIMFs, which can immobilize single strand DNAs as a non-fluorescent compound [4]. Fig. 3 (b) shows that PDIMFs are also a quencher in ODI-CL detection. However, the quenching constant ($K_q = 1.07$ ml/mg) of PDIMFs is about 20 times smaller than that ($K_q = 20.63$ ml/mg) of MWCNTs (see Scheme S1 and equations [22] to determine K_q shown in Supporting information). Thus, we selected PDIMFs to immobilize aptamer-conjugated TEX 615 to develop highly sensitive aptasensor capable of sensing trace levels of OTA based on the simple procedures shown in Fig. 4. Aptamer-conjugated TEX 615 immobilized on the surface of PDIMFs do not emit light due to the chemiluminescent resonance energy transfer (CRET) from aptamers excited by the CIEEL mechanism of ODI-CL reaction to PDIMFs, whereas aptamer-conjugated TEX 615 bound with OTA (G-quadruplex structure) emits red light.

3.3. Immobilization of aptamer-conjugated TEX 615 on the surface of PDIMFs

As shown in Table 1, I_{CL} immediately measured after aptamer was added in 1.5-ml centrifuge tube containing PDIMFs is about

27 times lower than that in aptamer only. However, I_{CL} after the 10-min incubation was about 23% lower than that immediately measured after mixing the mixture for 1 s using a vortex. I_{CL} measured after the longer incubation (e.g., 20-, 30-min) than 10-min was constant with that measured after 10-min incubation within an acceptable error range ($< 5\%$). Thus, most of aptamers were immediately immobilized on the surface of PDIMFs based on the π - π stacking interaction between ssDNA aptamers and PDIMFs (see Fig. 4). The result is consistent with that reported by Li and Sun [4]. Unfortunately, I_{CL} measured after the 10-min incubation is higher than the background (see Table 1) measured with the solution containing only PDIMFs because trace levels of free aptamers conjugated with TEX615, not bound with PDIMFs, are still in the solution. To develop a more sensitive ODI-CL aptasensor with the reduction of effect of free aptamers, the mixture was diluted. I_{CL} (1150 ± 55) of 20-time diluted solution was similar to the background measured in the absence of free aptamers. The result indicates that interference effect (e.g., enhancement of background) of free aptamer-conjugated TEX 615 not bound on PDIMFs was removed by the dilution.

OTA (125 nM) in Tris-HCl buffer solution (pH 8.5) was added in 20-, 40-, and 80-time diluted solution of the mixture prepared in Table 1. Then, they were incubated for 5 min at room temperature. Signal to background ratio ($S/B = 10 \pm 0.5$) determined with CL

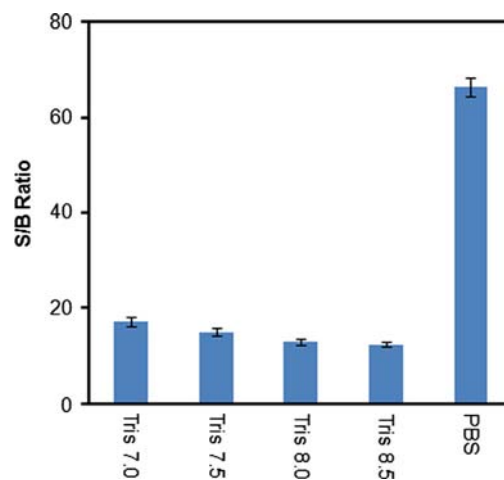


Fig. 5. Effect of buffer solution containing 625 nM OTA for the development of aptasensor with ODI-CL detection using aptamer-conjugated TEX 615 immobilized on the surface of PDIMFs.

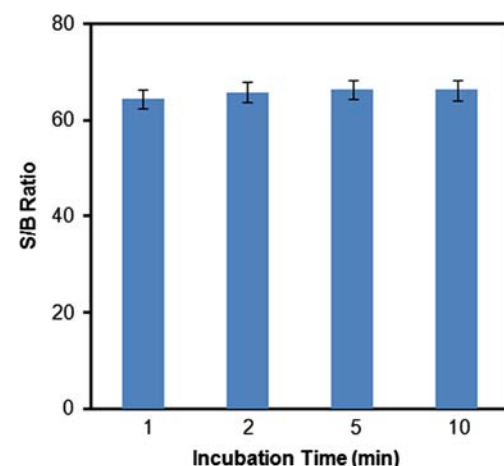


Fig. 6. Effect of incubation time to detect 625 nM OTA using aptamer-conjugated TEX 615 immobilized on the surface of PDIMFs.

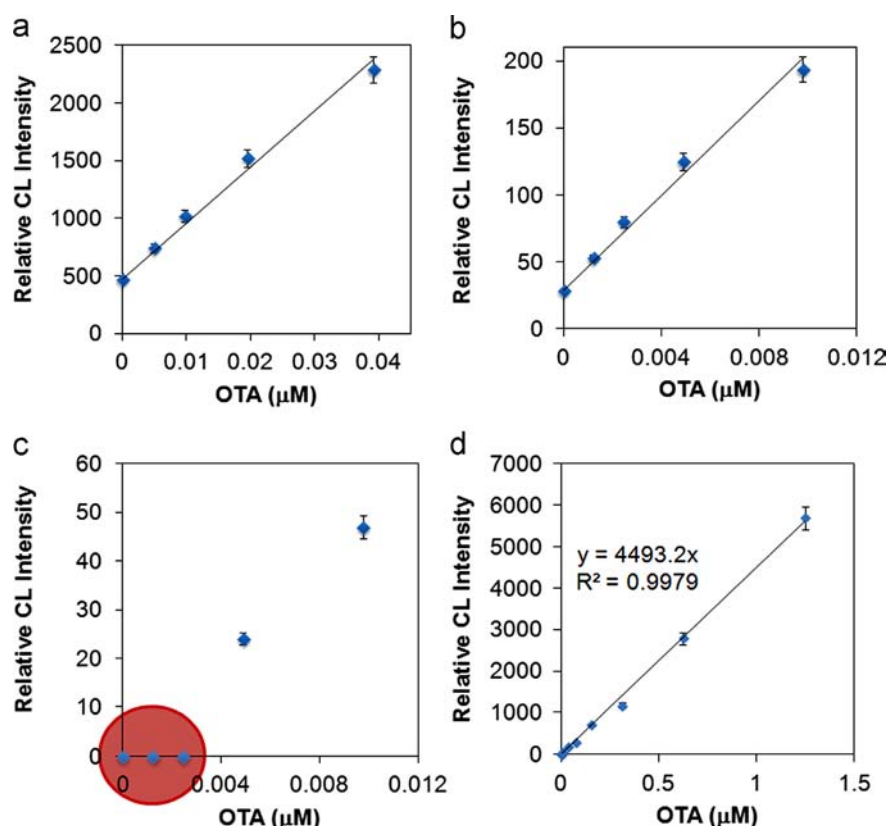


Fig. 7. Effect of background for the quantification of OTA in red wine using aptasensor with ODI-CL detection. In order to obtain calibration curves of (a)–(c), ODI solution used in Fig. 2 was diluted 2, 20, and 200 times in ethyl acetate. (d) is the wide calibration curve of (c). Controls containing different concentration of OTA was prepared PBS buffer with 1% red wine.

emission of aptamer-conjugated TEX 615 bound with OTA (G-quadruplex structure shown in Fig. 4) formed in the 80-time diluted solution was slightly smaller than those ($S/B = 12 \pm 0.4$ and 11 ± 0.7) in 20- and 40-time diluted mixtures. These results indicate that the concentration of aptamer-conjugated TEX 615 immobilized on the surface of PDIMFs existing in 80-time diluted solution was enough to rapidly quantify low concentration of OTA based on the procedures shown in Fig. 4.

3.4. Effect of buffer solution containing OTA in aptasensor with ODI-CL detection

To determine an appropriate buffer solution containing OTA added in a highly sensitive aptasensor with low background, OTA was prepared in five different buffers as shown in Fig. 5. OTA dissolved in each buffer was mixed with aptamer-conjugated TEX 615 immobilized on the surface of PDIMFs 80-time diluted in phosphate buffered saline (PBS). Then, the mixture was incubated for 5 min. S/B ratio shown in Fig. 5(a) was dependent on properties of buffer.

As shown in Fig. 5(a), S/B ratio in PBS buffer containing K^+ ions (pH 7.4) was higher than that in Tris–HCl buffer (pH 7.5) which do not contain K^+ ions. The result indicates that the binding interaction between OTA and aptamer in PBS buffer in the presence of K^+ ions is easier and faster than that in Tris–HCl buffer. It is consistent with results reported by two research groups that OTA rapidly binds with aptamer in the presence of K^+ [10] or Ca^{2+} [24,25]. Also, S/B ratio was dependent on pH of Tris–HCl buffer solution. S/B ratio in Tris–HCl buffer (pH 7) was higher than those in the rest Tris–HCl buffers (pH 7.5, 8, 8.5) because relative ODI-CL at neutral pH condition is stronger than that at basic pH condition [26].

Based on the results shown in Fig. 5, we selected PBS as a buffer to prepare OTA sample.

3.5. Effect of incubation time for the quantification of OTA using aptasensor with ODI-CL detection

Fig. 6 indicates that OTA in PBS rapidly interacts with aptamer-conjugated TEX 615 immobilized on the surface of PDIMFs. Aptamer-conjugated TEX 615 captured most of OTAs within 1 min. Thus, S/B ratio determined after 1-min incubation was the same as that obtained after 10 min of incubation. The results indicate that accuracy and precision of chemiluminescent aptasensor capable of rapidly quantifying OTA are independent of incubation time.

3.6. Role of background in aptasensor with ODI-CL detection for the quantification of OTA in red wine

As shown in Figs. 7 and S2 of Supporting information, the background of ODI chemiluminescent aptasensor operated with low concentration of ODI was lower than those generated with high concentration of ODI. Thus, ODI chemiluminescent aptasensor with low background generated under Fig. 7(b) condition was more sensitive than that with high background operated under Fig. 7(a) condition. In addition, S/B ratio to quantify a certain concentration of OTA under Fig. 7(b) was larger than that under Fig. 7(a). These results indicate that accuracy, precision, sensitivity and reproducibility of the former is better than those of the latter. For example, the limit of detection ($LOD = \text{background} + 3 \times \text{standard deviation}$) determined under Fig. 7(b) condition was 0.5 nM, whereas LOD under Fig. 7(a) was 3.9 nM. However, the sensitivity of background free ODI-CL aptasensor shown in Fig. 7

Table 2

Comparison between new aptasensors and conventional methods to quantify OTA in red wine or beer.

Method	Detector	Analytical time (min)	Dynamic range (nM) ^a	S/B ratio ^b	LOD (nM)	Reference
Aptasensor with high background (Fig. 7(a)) ^c	ODI CL	< 10	3.9–1200	108	3.9	This research
Aptasensor with low background (Fig. 7(b)) ^c	ODI CL	< 10	0.5–1200	518	0.5	
Aptasensor with no background (Fig. 7(c)) ^c	ODI CL	< 10	4.7–1200	n.d. ^f	4.7	
Aptasensor using Graphene Oxide ^e	Fluorescence	45	18.7–500	2	18.7	1
Aptasensor using single-walled CNTs ^d	Fluorescence	45	24.1–200	1.4	24.1	2
Competitive ELISA with HRP ^e	Fluorescence	280	5–25	N/A ^g	5.0	5
Competitive ELISA with HRP ^e	Electrochemical	150	1.7–248	N/A ^g	0.7	6
Competitive ELISA with ALP ^e	Electrochemical	150	0.7–24.8	N/A ^g	1.7	6
Direct Competitive ELISA with ALP ^e	Electrochemical	135	0.4–24.8	N/A ^g	0.4	7

^a From LOD.^b The ratio between signal measured to quantify the highest concentration of OTA under the dynamic range and background of each aptasensor.^c 1% Red wine in buffer.^d 1% Beer in buffer.^e 100% Red wine.^f Not determined because the background of aptasensor was zero.^g Not applicable because signal is exponentially decrease with the increase of OTA concentration.**Table 3**Recovery test of background free chemiluminescent aptasensor ($n=5$).

Sample 1 ^a	Sample 2 ^a	Expected ^a	Result ^a	Accuracy ^b	Precision ^b	Recovery ^b
4.9	19.5	12.2	13.6	11.5	4.5	111.5
39.1	156.3	97.7	102.2	4.4	3.2	104.4
312.5	1250	781.3	806.3	3.2	4.7	103.2

^a nM.^b %, Experimental condition was the same as that of Fig. 7(d).

(c) was not as good as those of Fig. 7(a) and (b) even though the former also has a wide calibration curve (See Fig. 7(d)). This is because the optical sensor can not detect dim light emitted from G-quadruplex structure, formed in the presence of lower OTA than 4.7 nM, after receiving energy from X based on CIEEL mechanism.

Table 2 shows that ODI-CL Aptasensor with lower background can quantify trace levels of OTA in red wine with various advantages. First, LODs of aptasensors with ODI-CL detection was lower than those of aptasensors with fluorescence detection as well as similar to those of complicated and time-consuming ELISAs using expensive antibody produced with the sacrifice of small animals. Second, the analytical time required to quantify of trace levels of OTA using aptasensors with ODI-CL detection is shorter than those using other methods. Third, the dynamic ranges of aptasensors with ODI-CL detection were wider than those of other methods. Fourth, S/B ratios of aptasensors with ODI CL detection were larger than those of aptasensors with fluorescence detection having relatively high background.

We conducted recovery tests of ODI-CL aptasensor under the conditions of Fig. 7(d). Each sample was prepared with the addition of a certain concentration of OTA in PBS buffer containing 1% red wine. Sample 1 (100 μ l) in Table 3 were mixed with sample 2 (100 μ l). Then, the expected concentration of each mixture (1:1 volume ratio of sample 1 and 2) shown in Table 3 was calculated. As shown in Table 3, Accuracy, precision, and recoveries of ODI chemiluminescent aptasensor were good within the statistically acceptable error range.

4. Conclusions

In summary, we studied for the first time the role of background in aptasensor with ODI-CL detection, capable of rapidly quantifying trace levels of OTA, with optimizations of various variables (e.g., the selection of micro- or nano-particles to immobilize free aptamer-conjugated fluorescent dye with less

quenching effect, the selection of fluorescent dye labeled with aptamer capable of emitting strong CL, the effect of buffer solution, the effect of ODI concentration). We confirmed that ODI-CL aptasensor with low background can rapidly quantify trace levels of OTA in a sample with excellent accuracy, precision, sensitivity, and reproducibility. Currently, various types of quadruplex aptamers (e.g.,), capable of capturing a specific target molecule in a sample with excellent selectivity, have been developed to be applied in various research fields such as biochemistry, clinical chemistry, food safety, molecular biology, and toxicology. Thus, if various types of G-quadruplexes formed after binding with targets do not interact with PDIMFs, ODI-CL aptasensor operated with the immobilization of ssDNAs on the surface of PDIMFs can be applied to various research areas as a new analytical sensor for quantifying trace levels of target molecule in a sample.

Appendix A. Supporting information

Supplementary data associated with this article can be found in the online version at <http://dx.doi.org/10.1016/j.talanta.2013.07.072>.

References

- [1] L.F. Sheng, J.T. Ren, Y.Q. Miao, J.H. Wang, E.K. Wang, *Biosens. Bioelectron.* 26 (2011) 3494–3499.
- [2] Z.J. Guo, J.T. Ren, J.H. Wang, E.K. Wang, *Talanta* 85 (2011) 2517–2521.
- [3] R. Freeman, J. Girsh, A.F.J. Jou, J.A.A. Ho, T. Hug, J. Darnedde, I. Willner, *Anal. Chem.* 84 (2012) 6192–6198.
- [4] H. Li, X. Sun, *Anal. Chim. Acta* 702 (2011) 109–113.
- [5] I. Bazin, N. Andreotti, A.I.H. Hassine, M.D. Waard, J.M. Sabatier, C. Gonzalez, *Biosens. Bioelectron.* 40 (2013) 240–246.
- [6] B. Prieto-Simon, M. Campas, J.-L. Marty, T. Noguer, *Biosens. Bioelectron.* 23 (2008) 995–1002.
- [7] L. Barthelmebs, A. Hayat, A.W. Limiadi, A.W.J.-L. Marty, T. Noguer, *Sens. Actuators B* 156 (2011) 932–937.
- [8] M. Tsunoda, K. Imai, *Anal. Chim. Acta* 541 (2005) 13–23.
- [9] J.A. Cruz-Aguado, G. Penner, *J. Agric. Food Chem.* 56 (2008) 10456–10461.
- [10] C. Yang, Y. Wang, J.-L. Marty, X. Yang, *Biosens. Bioelectron.* 26 (2011) 2724–2727.
- [11] A. Hayat, A. Sassolas, J.L. Marty, A. Radi, *Talanta* 103 (2013) 14–19.
- [12] J. Motoyoshiya, T. Maruyama, *Luminescence* 25 (2010) 181–182.
- [13] P.S. Park, T.H.D. Rho, Y.T. Kim, S.O. Ko, M.A. Schlautman, E.R. Carraway, J.H. Lee, *Chem. Commun.* 47 (2011) 5542–5544.
- [14] J.H. Lee, J.C. Rock, S.B. Park, M.A. Schlautman, E.R. Carraway, *J. Chem. Soc., Perkin Trans. 2* (2002) 802–809.
- [15] L.F.M. Cistato, F.H. Bartoloni, E.L. Bastos, W.J. Baader, *J. Org. Chem.* 74 (2009) 8974–8979.
- [16] H. Isobe, Y. Takano, M. Mitsutaka, S. Kuramitsu, K. Yamaguchi, *J. Am. Chem. Soc.* 127 (2005) 8667–8679.
- [17] J.H. Choi, Y.T. Kim, J.H. Lee, *Analyst* 135 (2010) 2445–2450.

- [18] J.H. Lee, J.Y.R. Rho, T.H.D. Rho, J.G. Newby, Biosens. Bioelectron. 26 (2010) 377–382.
- [19] R. Chong, J.E.R. Rho, H.J. Yoon, T.H.D. Rho, P.S. Park, Y.H. Kim, J.H. Lee, Biosens. Bioelectron. 32 (2012) 19–23.
- [20] R. Chong, J.E.R. Rho, H.J. Yoon, T.H.D. Rho, P.S. Park, J.Y. Park, L. Park, Y.H. Kim, J.H. Lee, Talanta 116 (2013) 403–408.
- [21] F.J. Alba, J.R. Daban, Luminescence 16 (2001) 247–249.
- [22] J.H. Lee, J. Je, A. Tartaglia, J. Hur, M.A. Schlautman, E.R. Carraway, J. Photochem. Photobiol. A 182 (2006) 28–32.
- [23] H. Cho, S. Lee, J.H. Lee, Analyst 137 (2012) 5368–5373.
- [24] G. Castillo, I. Lamberti, L. Mosiello, T. Hianik, Electroanalysis 24 (2012) 512–520.
- [25] I. Lamberti, L. Mosiello, T. Hianik, Chem. Sensors 1 (2011) 11.
- [26] J.H. Lee, J. Je, J. Hur, M.A. Schlautman, E.R. Carraway, Analyst 128 (2003) 1257–1261.